

View Article Online
View Journal

# Journal of Materials Chemistry A

Materials for energy and sustainability

# Accepted Manuscript

This article can be cited before page numbers have been issued, to do this please use: A. Petrongari, L. Desiderio, A. Pierini, S. Brutti, E. Bodo and M. Giustini, *J. Mater. Chem. A*, 2025, DOI: 10.1039/D5TA04150C.



This is an Accepted Manuscript, which has been through the Royal Society of Chemistry peer review process and has been accepted for publication.

Accepted Manuscripts are published online shortly after acceptance, before technical editing, formatting and proof reading. Using this free service, authors can make their results available to the community, in citable form, before we publish the edited article. We will replace this Accepted Manuscript with the edited and formatted Advance Article as soon as it is available.

You can find more information about Accepted Manuscripts in the <u>Information for Authors</u>.

Please note that technical editing may introduce minor changes to the text and/or graphics, which may alter content. The journal's standard <u>Terms & Conditions</u> and the <u>Ethical guidelines</u> still apply. In no event shall the Royal Society of Chemistry be held responsible for any errors or omissions in this Accepted Manuscript or any consequences arising from the use of any information it contains.



Open Access Article. Published on 21 October 2025. Downloaded on 10/27/2025 3:04:47 AM.

This article is licensed under a Creative Commons Attribution-NonCommercial 3.0 Unported Licence

View Article Online DOI: 10.1039/D5TA04150C

# **ARTICLE**

# Deciphering the role of LiBr as redox mediator in Li-O2 Aprotic Batteries

Received 00th January 20xx, Accepted 00th January 20xx

DOI: 10.1039/x0xx00000x

Angelica Petrongari [a], Lucrezia Desiderio [a], Adriano Pierini [a], Enrico Bodo [a], Mauro Giustini [a], Sergio Brutti [a,b,c]

Lithium-oxygen batteries (Li-O2) represent a highly promising category of energy storage systems, primarily owing to their elevated theoretical energy density. Nevertheless, their effective deployment is significantly impeded by challenges such as inadequate reversibility and the presence of undesirable parasitic reactions. Recent investigations have turned to redox mediators, specifically lithium bromide (LiBr), as a potential solution to improve reaction kinetics and minimize overpotentials in these systems. This research presents a comprehensive analysis of the effects of three distinct solvents - dimethoxyethane (DME), tetraethylene glycol dimethyl ether (TEGDME), and dimethyl sulfoxide (DMSO) - on both the electrochemical performance and reaction mechanisms of LiBr-mediated lithium-oxygen cells. The findings indicate that singlet oxygen (¹O₂), which contributes to cell degradation through secondary reactions, is generated only in the presence of TEGDME as the electrolyte solvent. In contrast, while both DME and DMSO enable oxygen evolution without forming singlet oxygen, only DME exhibits chemical stability under the operating conditions of LiBr-mediated Li-O₂ cells. Furthermore, a comparative analysis of the redox mediation effects arising from lithium iodide (LiI) and LiBr across various solvent environments reveals that the activation of the singlet oxygen release pathway occurs when the Lewis acidity and basicity of the oxidized redox mediator and the solvent are aligned: e.g. when both behave as weak acids/bases or as strong acids/bases. This study elucidates the nuanced interactions between solvents and redox mediators, thereby contributing to the advancement of more efficient lithium-oxygen battery systems.

#### Introduction

Aprotic Li- $O_2$  batteries are considered a promising technology to address the increasing demand of energy storage systems. These devices can potentially deliver outstanding performances thanks to their gravimetric energy density (up to 3458 Wh/kg with  $\text{Li}_2O_2$  as discharge product) and high operating potential (i.e. 2.96 V vs.  $\text{Li}^+/\text{Li}^0)^1$ . The redox processes involved in the functioning of a  $\text{Li}^-O_2$  cell are the dissolution (discharge) and deposition (charge) of lithium at the lithium metal anode; the Oxygen Reduction Reaction (ORR, discharge) and Oxygen Evolution Reaction (OER, charge) at the carbonaceous cathode. In aprotic electrolytes, ORR and OER lead to the formation and dissolution, respectively, of the non-conductive solid lithium peroxide<sup>2</sup>.

Some key drawbacks must be faced before achieving the practical implementation of these systems: in particular, the high overpotentials required during the charge process, i.e. the oxidation of lithium peroxide to molecular oxygen, must be efficiently lowered to avoid undesired processes that lead to early performance decay of the cell<sup>3,4</sup>. Among the strategies to

suppress singlet oxygen ( $^1O_2$ ) in Li-O $_2$  batteries, quenching mechanisms have been explored. Molecules such as triphenylamine (TPA) and its brominated derivative can capture  $^1O_2$  and convert it to ground-state oxygen, effectively reducing parasitic reactions and improving battery stability $^{5,6}$ . Another effective method to avoid singlet oxygen production is to introduce soluble catalysts named Redox Mediators (RMs), which are currently being explored and proposed in literature to favour the oxidation of  $\text{Li}_2O_2$  at lower overpotentials and preserve the cell components from degradation $^{7,8}$ . RMs are oxidized at the cathode surface and then diffuse to  $\text{Li}_2O_2$  deposits where they oxidize the peroxide anion to molecular oxygen, acting as electron carriers and allowing the lowering of the charge potential $^9$ .

Adding lithium halides, LiX, to the electrolyte solution is a promising and cost-effective strategy to employ the redox couples of halide species, in particular X-/X<sub>3</sub>- and X<sub>3</sub>-/X<sub>2</sub>, as redox mediators<sup>10</sup>. Lil is a widely studied RM that showed interesting results<sup>11,12</sup>, despite implying also additional concerns for the stability of cell components<sup>13</sup>. More recently, LiBr was also proposed as electrolyte salt and redox mediator by Kwak et al.<sup>14</sup>, that highlighted some advantages of this RM against Lil: a higher oxidizing power due to the higher standard potential of the redox couple Br-/Br<sub>3</sub>-; a more efficient formation of Li<sub>2</sub>O<sub>2</sub> during discharge and little to none competition between bromide chemistry and ORR/OER. These differences are consistent with our findings reported in reference 16, where Lil

<sup>[</sup>a] Department of Chemistry, Sapienza University of Rome, P.le Aldo Moro 5, Rome, 00185, Italy.

<sup>[</sup>b] CNR-ISC, Consiglio Nazionale delle Ricerche, Istituto dei Sistemi Complessi, Rome, 00185. Italv.

<sup>[</sup>c] GISEL – Centro di Riferimento Nazionale per i Sistemi di Accumulo Elettrochimico di Energia, Florence, 50121, Italy.

was tested in the same solvent systems used in the present study for LiBr. In Kwak et al.'s report, LiBr performance was particularly promising when using diglyme = diethylene glycol dimethyl ether) as electrolyte solvent, while a decay of the cell performance along with a worsening of the charge/discharge overpotentials was observed using TEGDME as solvent<sup>14</sup>. This behaviour deviates from that observed in the case of Lil<sup>11</sup>, and the fundamental origin of such a different performance outcome when varying between very similar solvents was not further explained up to now. Basing on Pierini et al.'s calculations<sup>15</sup>, we hypothesized that, similarly to Lil case, the promotion of singlet oxygen release due to the introduction of the RM could be involved. The oxidation of a cluster of (Li<sub>2</sub>O<sub>2</sub>)<sub>4</sub> by Br<sub>3</sub>- resulted thermodynamically favoured in both highly polarity solvents like DMSO and ethereal solvents<sup>15</sup>, suggesting that in the case of LiBr singlet oxygen generation could be favoured also in low-polarity media, in contrast with the case of Lil.

In fact, in a previous study<sup>16</sup>, we observed that the use of Lil coupled with a high-polarity solvent like DMSO, where the oxidation of  $Li_2O_2$  by  $I_3$  corresponds to a  $\Delta G < 0^{15}$ , leads to a significative increase of the amount of <sup>1</sup>O<sub>2</sub> evolved during the oxidation of Li<sub>2</sub>O<sub>2</sub> by the redox mediator. The implications of using LiBr on the degradative processes in the Li-O<sub>2</sub> cell need to be widely explored in order to design a proper electrolyte formulation to maximize the performance of this promising RM. With this aim, we carried out a study employing LiBr 200 mM + LiTFSI 1M in monoglyme (TEGDME)/dimethylsulfoxide (DME)/tetraglyme solvents, to find out the fundamental origin of different performance outcomes within the same class of solvents and same range of polarity in the case of DME and TEGDME ( $\varepsilon_r = 7.2$ and 7.4, respectively<sup>17,18</sup>), and to highlight also the effect of a sharp change in polarity using DMSO ( $\varepsilon_r$  = 46.8<sup>19</sup>). The 200 mM concentration of LiBr was chosen to ensure the best reversibility of the ORR/OER processes, as indicated by the preliminary tests reported in Figure S1.

## **Materials and Methods**

#### Electrolytes.

High-purity 1,2-dimethoxyethane (monoglyme; DME) [anhydrous, 99.5%, inhibitor-free], tetraglyme (TEGDME) [tetraethylene glycol dimethyl ether, anhydrous, ≥99%] and dimethyl sulfoxide (DMSO) [Sigma-Aldrich, anhydrous, ≥99%] were purchased from Sigma-Aldrich and dried over 4 Å molecular sieves for at least 1 week before use. Battery grade LiTFSI (lithium bis(trifluoromethanesulfonyl)imide extra dry <20 ppm of  $H_2O$ , Solvionic) was used as received. LiBr (Reagent-Plus®, ≥ 99%, Sigma-Aldrich) was dried under vacuum at 50°C for 48h before use. Electrolyte solutions of LiTFSI 1M + LiBr 200 mM in DME/TEGDME/DMSO were prepared in an Ar filled glovebox (Iteco Eng SGS-30,  $H_2O$  < 0.1 ppm).

#### **Electrochemical Measurements.**

An EL-CELL ECC-Air test cell was used to perform electrochemical experiments. The internal configuration of the cell employed for all the measurements is the following: Li(-

)/Separator-Electrolyte/GDL(+)/Ni Foam/Gaseous Q2 (1 bar) A glass fiber separator (Whatman, 1.55 ନମନା: thickine ୨୭,୮184 ନନନ diameter) soaked in 1 M LiTFSI + 200 mM LiBr in DME/TEGDME/DMSO electrolytes was employed. 15 mm discs of a commercial carbonaceous Gas Diffusion Layer (GDL, MTI Corp.) were used as cathodes. A metallic lithium foil was used as anode. A nickel foam disc (16 mm diameter) was used above the GDL to ensure a homogeneous O2 impregnation. Cell assembly was performed in an Ar filled glovebox (Iteco Eng SGS-30,  $H_2O < 0.1$  ppm). The Li-O<sub>2</sub> cells were filled with pure O<sub>2</sub>, setting a static final pressure of 2.0 bar in the cell volume (head space 4.3 cm<sup>3</sup>). Galvanostatic cycling tests were run on (-)Li<sup>0</sup>|LiTFSI 1 M + LiBr 200 mM in DME|GDL(+), (-)Li<sup>0</sup>|LiTFSI 1 M + LiBr 200 mM in TEGDME | GDL(+) and (-)Li<sup>0</sup> | LiTFSI 1 M + LiBr 200 mM in DMSO|GDL(+) cells at 0.1 mA cm<sup>-2</sup> with a limited capacity of 0.2 mAh cm<sup>-2</sup> and cut-off potentials of 2.0 and 3.6 V vs Li<sup>+</sup>/Li<sup>0</sup>, using a Maccor Series 4000 Battery Test System.

#### Ex-situ experiments.

The fluorescent probe DMA [9,10-dimethylanthracene, 99%] and Bromine (Br<sub>2</sub>, Suprapur®, 99.9999%) were purchased from Sigma-Aldrich and used as received. A set of reference DMA solutions, at the concentrations of 0.5-1-2.5-5-7.5 and 10  $\mu$ M, was prepared in each solvent (DME/TEGDME/DMSO) for the construction of the calibration lines. The reaction solutions were prepared in each solvent according to the following scheme:

- <u>Solution A:</u> 5.15 mg of 9,10-dimethylanthracene were dissolved in 5 mL of the chosen solvent to obtain a 5 mM solution. The solution was then diluted with the same solvent to 0.2 mM of DMA.
- <u>Solution B:</u> 10  $\mu$ L of pure Br<sub>2</sub> and 33.7 mg of dry LiBr were added to 4.85 mL of the chosen solvent to obtain a 40 mM solution of Br<sub>3</sub>. The solution was then diluted with the same solvent to 0.2 mM.

Equal volumes of solutions A and B were mixed to obtain a 0.1 mM solution of both Br $_3$ - and DMA. A portion of the as-prepared solution was further diluted 10x and its fluorescence and UV spectra were measured as reference before adding Li $_2$ O $_2$ . Excess Li $_2$ O $_2$  was added to the other portion of the A+B solution to perform Li $_2$ O $_2$  oxidation by Br $_3$ - in presence of a 1:1 quantity of DMA as singlet oxygen trap, then the final solution was diluted 10x and its fluorescence and UV spectra were recorded. The preparation of both the reference and the reaction solutions was carried out under Ar atmosphere in a MBRAUN UniLab glovebox [H $_2$ O, O $_2$   $\leq$  1 ppm].

The measurements were carried out in sealable Hellma quartz fluorescence cuvettes 117104F-10-40, to prevent the exposure of the solutions to air moisture and oxygen. Fluorescence measurements were performed with a Fluoromax-2 spectrofluorometer (Jobin Yvon-Spex), in the range 392-600 nm with an excitation wavelength of 388 nm (slits 1.1/1.1 nm) and at a temperature of 25°C. UV spectra were recorded with a Varian Cary 5E UV-Vis spectrophotometer. Sealable fluorescence quartz cuvettes were also employed for the acquisition of Raman spectra.

Spectra of the 40 mM solution of  $Br_{3}^{-}$  before and after adding  $Li_2O_2$  were recorded in TEGDME and DMSO as solvents. Raman

Journal Name ARTICLE

measurements were carried out with a DILOR LabRam confocal micro-Raman equipped with a He-Ne laser source at 632.7 nm. **Computational details**.

Simulations of Raman spectra of  $Br_3^-$  and  $Br_2$  were carried out using density functional theory (DFT) at M062X/def2-TZVP level. Simulations of FTIR spectra of dimethyl sulfide and methanesulfonic acid were carried out by DFT at wB97X/def2-TZVPP<sup>20</sup>, NoFrozenCore level of theory, with the Orca package distribution,version  $5.03^{21}$ .

It is important to underline that in the case of the LLSR of Ellings redox mediator, the impact of the  $I_3$  accumulation is larger while it is almost negligible in the case of LiBr mediation. This aspect indicates that LiBr offers better performance in ethereal solvents, thanks to the very high overpotentials required for the reduction of  $Br_3$  on the carbon cathode that make this process non-competitive with the ORR during discharge. On passing we would like to stress that, despite the technological validation of this electrolyte formulation for Li-O<sub>2</sub> necessarily requires a much more extended cycling in terms of limiting

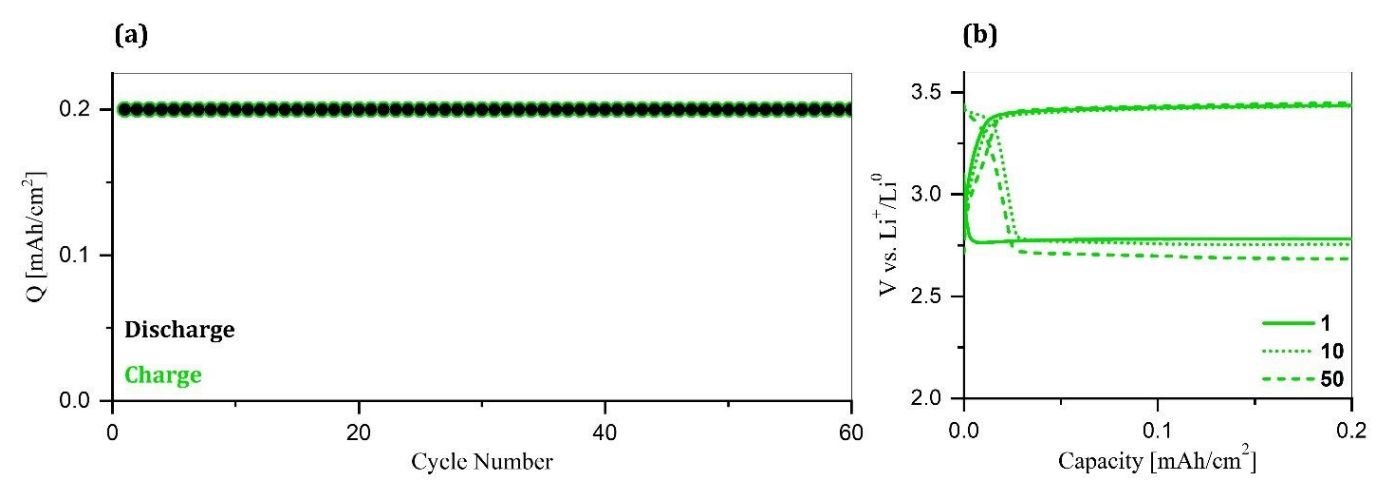


Figure 1. (a) Discharge/Charge capacities achieved by a Li-O<sub>2</sub> cell with LiTFSI 1M + LiBr 200 mM in DME electrolyte, cycled at J=0.1 mA/cm<sup>2</sup>, Q<sub>lim</sub>=0.2 mAh/cm<sup>2</sup>, V<sub>cut-off</sub>=2.0-3.6 V vs. Li<sup>+</sup>/Li<sup>0</sup>, for 60 cycles. (b) Voltage profiles of the 1<sup>st</sup>, 10<sup>th</sup> and 50<sup>th</sup> cycle

# Results

This article is licensed under a Creative Commons Attribution-NonCommercial 3.0 Unported Licence

Open Access Article. Published on 21 October 2025. Downloaded on 10/27/2025 3:04:47 AM

#### LiBr redox mediation in DME

When charged up to 3.6 V with no limit capacity (Figure S1b), the Li-O<sub>2</sub> cell containing LiTFSI 1M + LiBr 200 mM in DME shows a charge profile closely matching the discharge, indicating good reversibility and efficient utilization of the redox mediator under these conditions. Moving to prolonged cycling conditions, the charge/discharge capacities achieved during the galvanostatic cycling of the same cell formulation with a limited capacity of 0.2 mAh/cm<sup>2</sup> at J = 0.1 mA/cm<sup>2</sup> are reported in Figure 1a. This electrolyte formulation allows a stable functioning of the LiBr-mediated cell, with an excellent reversibility of ORR/OER for at least 60 cycles. In line with this, the potential curves reported in Figure 1b indicate both a good discharge profile and a low-overpotential, stable charge performance. Only after 50 cycles a mild worsening of the discharge process is observed, as indicated by the higher overpotential at which the 50th discharge takes place, likely due to a reduced oxygen concentration at the reaction interface caused by cumulative minor irreversibilities. The slight shift of the discharge plateau towards higher capacities observed in the 10<sup>th</sup> and 50<sup>th</sup> discharges is likely owed to a moderate accumulation of Br<sub>3</sub>- during charge, which is by consequence reduced in correspondence with the very early stages of discharge at higher potentials than 2.75 V (i.e. the ORR onset).

current/capacities and cycle number, here our goal is to demonstrate the fundamental behaviour of LiBr as redox mediator in three different solvent media. In this respect the presented galvanostatic tests, even if limited to 60 cycles, offer a solid experimental basis to prove in which chemical environments LiBr drives or limits parasitic degradation reactivities. This experimental validation aims at consolidating our hypothesis that redox mediators and electrolytes are strongly interplayed and the impact of solvation on the thermodynamics, and kinetics, of redox mediation is not banal

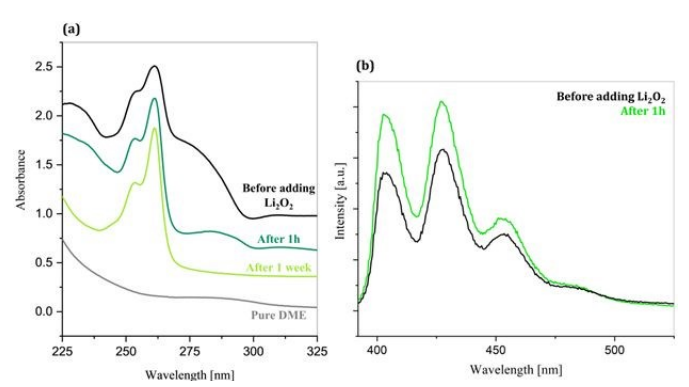


**Figure 2.** (a) UV spectra of pure DME (grey), and a solution of Br<sub>2</sub> 10  $\mu$ M + LiBr 40  $\mu$ M +DMA 10 $\mu$ M in DME before (black) and after (1h, dark green and 1week, light green) adding excess Li<sub>2</sub>O<sub>2</sub>. (b) Fluorescence spectra of a solution of Br<sub>2</sub> 10  $\mu$ M + LiBr 40  $\mu$ M + DMA 10 $\mu$ M in DME before (black) and after (green) adding excess Li<sub>2</sub>O<sub>2</sub>.

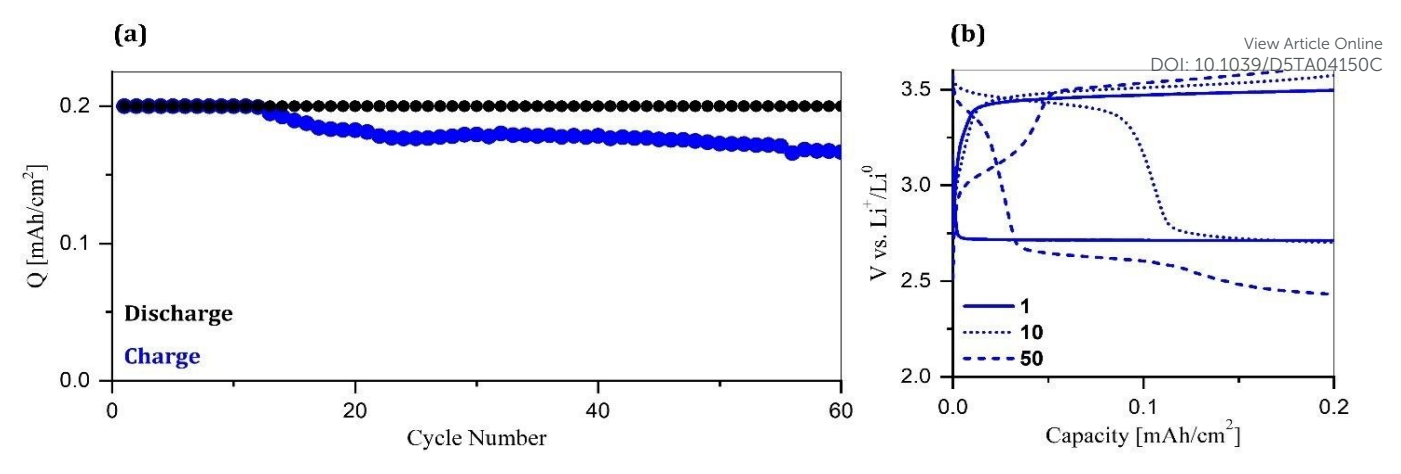


Figure 3. (a) Discharge/Charge capacities achieved by a Li-O<sub>2</sub> cell with the LiTFSI 1M + LiBr 200 mM in TEGDME electrolyte, cycled at J=0.1 mA/cm<sup>2</sup>,  $Q_{lim}=0.2$  mAh/cm<sup>2</sup>,  $V_{cut-off}=2.0-3.6$  V vs. Li<sup>+</sup>/Li<sup>0</sup> for 60 cycles. (b) Voltage profiles of the 1st, 10th and 50th cycle.

and cannot be fully explained by simple considerations starting from the acceptor/donor numbers of solvents. The good stability of the electrochemical performance of LiBr in DME suggests that this electrolyte formulation leads to limited parasitic chemistries and the possible suppression of <sup>1</sup>O<sub>2</sub> release beyond the quantities expected by the Boltzmann distribution, as calculated in Eq. S1. To confirm this hypothesis, an ex-situ study on the oxidation of Li<sub>2</sub>O<sub>2</sub> by Br<sub>3</sub><sup>-</sup> in DME was performed. Excess Li<sub>2</sub>O<sub>2</sub> was added to a 0.1 mM solution of Br<sub>3</sub>- in DME, in presence of 0.1 mM of DMA (the <sup>1</sup>O<sub>2</sub> trap). The reaction solution was then diluted to 0.01 mM in order to measure its UV and fluorescence spectra. Simultaneously, another aliquot of the initial solution was diluted to 0.01 mM (of Br<sub>3</sub><sup>-</sup> and DMA) and its UV and fluorescence spectra were measured as a reference of the spectral response of the solution before adding Li<sub>2</sub>O<sub>2</sub>. Figure 2a illustrates the UV spectra of the reaction solution before adding Li<sub>2</sub>O<sub>2</sub> and after 1h and 1 week. The baseline of pure DME is reported as blank. The UV signal of  $Br_3^-$  is localized at  $\sim 280$ nm: this position is assigned from the comparison with the shape and position of Br<sub>3</sub>- UV signal in aqueous solution observed in literature <sup>23</sup>. After 1 hour from adding Li<sub>2</sub>O<sub>2</sub>, a sharp decrease of the Br3- signal can be observed, hinting its consumption in the oxidation reaction with lithium peroxide. The complete disappearance of the Br3- -related signal is observed after 1 week from the onset of the reaction. The UV spectral response during the ongoing of the Li<sub>2</sub>O<sub>2</sub> oxidation by Br<sub>3</sub>- in DME highlights that not only is the reaction spontaneous but also occurs with relatively fast kinetics. It is worth mentioning that in the case Lil was used as RM, the oxidation of Li<sub>2</sub>O<sub>2</sub> in glymes is either not spontaneous<sup>15</sup> or strongly kinetically hindered<sup>12</sup>, while in the case of LiBr the analogous reaction results thermodynamically favoured from both theoretical calculations<sup>15</sup> and experimental evidence. Additionally, the Li<sub>2</sub>O<sub>2</sub> oxidation by Br<sub>3</sub>- in DME occurs without the evolution of <sup>1</sup>O<sub>2</sub>, as indicated by the comparison of DMA fluorescence spectra before and after adding Li<sub>2</sub>O<sub>2</sub> (Figure 2b). In fact, the increase in the fluorescence signal of DMA observed after adding Li<sub>2</sub>O<sub>2</sub> was demonstrated owed to an interaction between DMA and Li<sub>2</sub>O<sub>2</sub> only, with no contribution of the OER reaction mediated by Br<sub>3</sub>- to the intensity variation of the DMA

spectrum. When excess  $Li_2O_2$  is added to a 10  $\mu$ M solution of DMA in DME (Figure S2), the same increase in intensity is observed (see Table S1).

#### LiBr redox mediation in TEGDME

LiBr performance as redox mediator in TEGDME was firstly studied by Kwak et al.14, that already observed the worsening of the cell operation in this solvent respect to the shorter-chain diglyme. The observations discussed in the previous paragraph for DME as battery solvent are in line with the picture that emerges from Kwak et al.'s work. Overall, it appears that both DME and diglyme (DEGDME), which differ for a -O-(CH<sub>2</sub>)<sub>2</sub>- unit only, are suitable solvents for LiBr employement, while earlier performance decay is to be expected for longer chain glymes as TEGDME. This marked performance difference within the same class of solvents is peculiar of LiBr and was not observed in the case of Lil, nor for many other RMs<sup>24</sup>. In Figure 3, the electrochemical behaviour of a Li-O<sub>2</sub> cell containing LiTFSI 1M + LiBr 200 mM in TEGDME as electrolyte, cycled at J = 0.1 mA/cm<sup>2</sup>  $Q_{lim} = 0.2 \text{ mAh/cm}^2 \text{ between } 2.0 \text{ and } 3.6 \text{ V vs. Li}^+/\text{Li}^0, \text{ is reported.}$ Early failure of the charge process is observed starting from

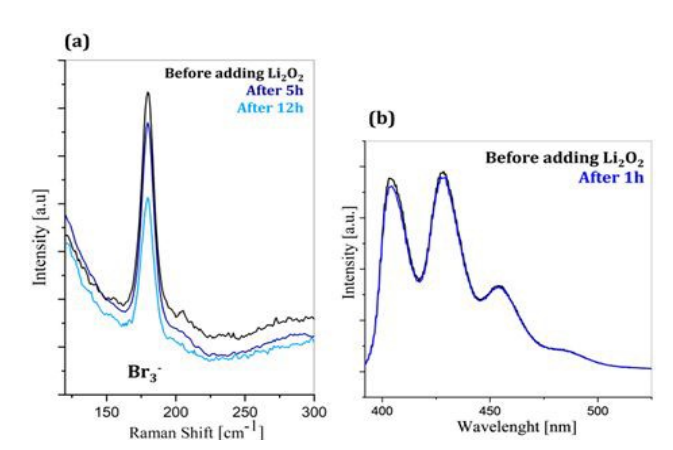


**Figure 4.** (a) Raman spectra of a solution of  $Br_3^-$  40 mM in TEGDME before adding excess  $Li_2O_2$ , after 5 hours (dark blue) and after 12 hours (light blue). (b) Fluorescence spectra of DMA before (black) and after 1 hour (blue) of adding  $Li_2O_2$  to the reaction solution of 0.1 mM  $Br_3^-$  + 0.1 mM DMA.

Journal Name ARTICLE

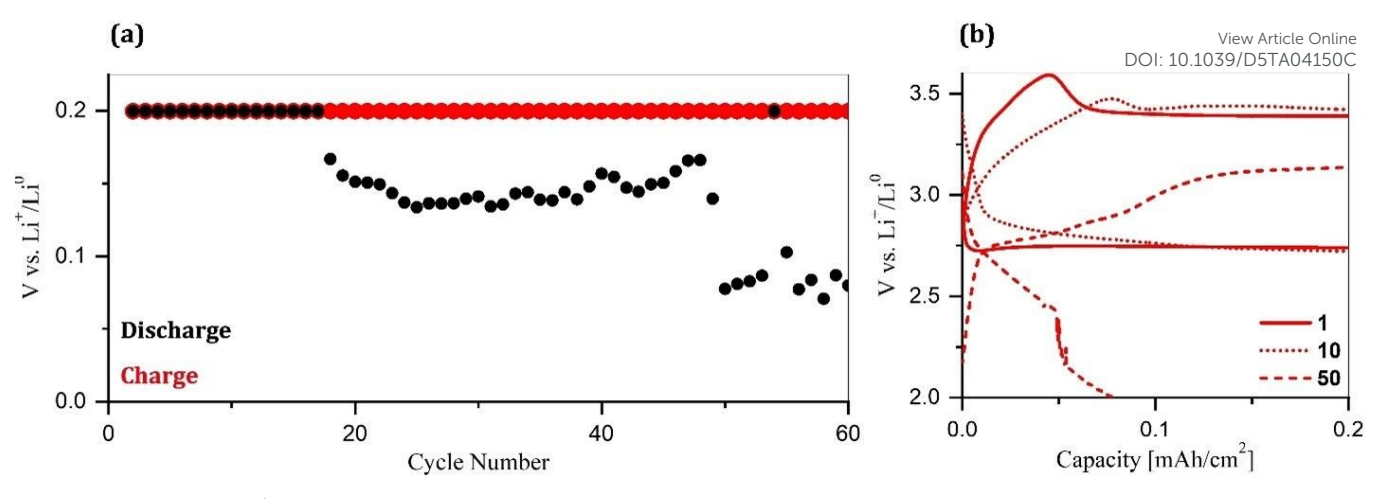


Figure 5. (a) Discharge/Charge capacities achieved by a Li- $O_2$  cell with the LiTFSI 1M + LiBr 200 mM in DMSO electrolyte, cycled at J=0.1 mA/cm<sup>2</sup>,  $Q_{lim}$ =0.2 mAh/cm<sup>2</sup>,  $V_{cut-off}$ =2.0-3.6 V vs. Li<sup>+</sup>/Li<sup>0</sup> for 60 cycles. (b) Voltage profiles of the 1<sup>st</sup>, 10<sup>th</sup> and 50<sup>th</sup> cycle.

cycle 12, from which the charge capacities continuously decrease (Figure 3a). The charge/discharge potential profiles shown in Figure 3b highlight the occurrence of critical parasitic chemistries: at the 10th cycle the participation of Br redox to the discharge capacity is extended to almost half of the total capacity, indicating that accumulation of Br<sub>3</sub>-during charge due to inefficient redox mediation is occurring. At the 50th cycle, a three-plateau discharge profile is observed. The first plateau at  $\sim$  3.4 V, which is related to excess  $Br_3^-$  reduction, is less extended than at the 10th discharge, however the ORR-related plateau at  $\sim$  2.7 V is shorter due to the presence of a third plateau at ~ 2.4 V, hinting that additional undesired processes are occurring alongside ORR. Observing the charge profiles, it appears that at the 10<sup>th</sup> charge only an increase in overpotential occurred, while a radical change in the electrochemical process is evident at the 50th cycle.

Such differences between the performance outcomes in DME and TEGDME may indicate that, despite the identical class of ethereal solvents, the 1O2 evolution channel activates in the solvent, i.e. TEGDME, that has a slightly larger dielectric constant and a slightly smaller acceptor number. The ex-situ experiments performed to understand the fundamentals of LiBr mediation in TEGDME are reported in Figure 4. When the reaction solution (40 mM Br<sub>3</sub>- + 40 mM DMA + excess Li<sub>2</sub>O<sub>2</sub> in TEGDME) was monitored over time by Raman spectroscopy, the consumption of Br<sub>3</sub><sup>-</sup> was confirmed (Figure 4a): a monotone decrease in the Raman Br<sub>3</sub><sup>-</sup> signal intensity centered at 175 cm<sup>-</sup> <sup>1</sup> is evident, strongly indicating that the oxidation of Li<sub>2</sub>O<sub>2</sub> has occurred. The assignment of the peak at 175 cm<sup>-1</sup> to LiBr<sub>3</sub> is confirmed by both literature references<sup>10</sup> and theoretical calculations (Figure S3). In Figure 4b, the fluorescence spectra of the singlet oxygen trap DMA before and after adding Li<sub>2</sub>O<sub>2</sub> in the reaction solution of  $\rm Br_{3}^{\scriptscriptstyle -}$  0.1 mM + DMA 0.1 mM in TEGDME are reported. A decrease of the fluorescence intensity indicates that part of the DMA in solution reacted with <sup>1</sup>O<sub>2</sub> forming the non-fluorescent DMA-endoperoxide.

From the calibration plot reported in Figure S4, it was possible to estimate that the amount of DMA that reacted with  $^1O_2$  was around 1.9% of the initial concentration. The 1:1 reaction

stoichiometry between DMA and 1O2, in forming DMAendoperoxide, therefore implies that at least  $\sim$  1.9% of the total molecular oxygen evolved in its singlet state. This result is comparable with that obtained for LiI redox mediation in DMSO reported in an our previous study<sup>16</sup> and demonstrates that also LiBr is able to open an alternative pathway for <sup>1</sup>O<sub>2</sub> evolution enabling its production far beyond the quantities expected from the Boltzmann distribution. Apparently, the key difference lies in the interplay between polarity (dielectric constant) and the Lewis acidity (acceptor number) of the solvent and the Lewis basicity of the redox mediator. Lil is the precursor of the strong Lewis base I3- and it leads to 1O2 generation only in a highpolarity solvent, DMSO, that is a strong Lewis acid with large acceptor number. In a low polarity/weak Lewis acid solvent like TEGDME, Lil mediates a <sup>1</sup>O<sub>2</sub>-free Li<sub>2</sub>O<sub>2</sub> oxidation. On the contrary LiBr is the precursor of the weak Lewis base Br<sub>3</sub>-, and activates the release of singlet oxygen in a low-polarity solvent, TEGDME, that is a weak Lewis acid, whereas in DME, a low polarity solvent but with an intermediate Lewis acidity (i.e. acceptor number intermediate between TEGDME and DMSO) the Li<sub>2</sub>O<sub>2</sub> oxidation mediated by LiBr is <sup>1</sup>O<sub>2</sub>-free.

#### LiBr redox mediation in DMSO

A different behaviour of LiBr-mediated Li-O<sub>2</sub> batteries is observed when DMSO is used as electrolyte solvent. In Figure 5 are reported the cycling performances of a Li-O<sub>2</sub> cell with LiTFSI 1M + LiBr 200 mM in DMSO. Already starting from the 18<sup>th</sup> cycle (Figure 5a), the discharge process becomes inefficient, likely due to the lack of molecular oxygen in the cell head compartment. The scarcity of oxygen supply may derive from an inefficient charging process, as can be deduced by the shape of the charge potential profiles of the first cycles (Figure 5b), that indicate the onset of a parasitic process activated at  $\sim 3.6$  V. Basing on the observation of the preliminary electrochemical tests with no limit capacity (Figure S5), it appears that this process involves not only the oxidations of Br to Br<sub>3</sub> and Li<sub>2</sub>O<sub>2</sub> to O<sub>2</sub>, but also the oxidation of electrolyte components,

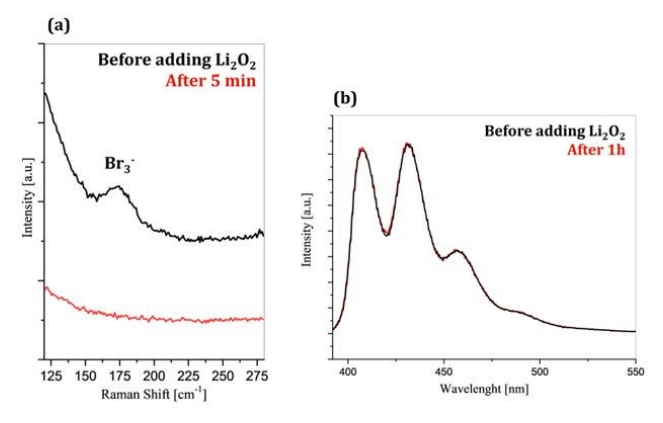


**Figure 6.** (a) Raman spectra of a solution of  $Br_3^- 40$  mM in DMSO before (black) and after 5 minutes (red) from adding excess  $Li_2O_2$ . (b) Fluorescence spectra of DMA before (black) and after 1 hour (red) from adding  $Li_2O_2$  to the reaction solution of 0.1 mM  $Br_3^- + 0.1$  mM DMA.

hindering the actual OER. As a consequence, the accumulation of Br<sub>3</sub>- (or Br<sub>2</sub>) occurs cycle by cycle due to the progressive lack of Li<sub>2</sub>O<sub>2</sub> formed during discharge. We can speculate that the high polarity of DMSO allows the involvement of the second redox couple of LiBr within the potential window employed for the galvanostatic cycling of the cell, i.e. 2.0-3.6 V vs. Li<sup>+</sup>/Li<sup>0</sup>, with the oxidation of  $Br_3^-$  to  $Br_2$  occurring at  $\sim 3.6$  V. In fact, it was observed that this reaction occurs at lower potential in DMSO (3.9 V) than in ethers (4.1 V)9 in Ar atmosphere, and since these values are further lowered in presence of O<sub>2</sub> <sup>14</sup> it is reasonable that the  $Br_3$ -/ $Br_2$  oxidation is the process occurring at  $\sim 3.6 \text{ V}$  in the charge profiles reported in Figure 5b. Qualitatively, it was observed that, upon the recovering and washing of the cathodes, only the one cycled in DMSO led to the colouring of the fresh solvent to orange (Figure S6), supporting the presence of high quantities of Br2 in the electrolyte after the cycling procedure. Once formed, Br<sub>2</sub> is able to decompose DMSO to dimethyl sulfide, formaldehyde and methanesulfonic acid, according to the scheme elucidated by Aida et al.<sup>25</sup>.

Basing on these evaluations, it is likely that the short cycle life of the Li-O<sub>2</sub> cell cycled with the DMSO-based electrolyte can be safely attributed to the chemical instability of DMSO in the presence of Br<sub>2</sub>. Although the production of  $^1O_2$  is in this case reasonable due to the theoretical predictions $^{15}$ , it has to be kept in mind that the oxidizing power of Br<sub>2</sub> towards the solvent and the Li salt may also be the most relevant aspect leading to cell failure.

The ex-situ experiments performed to study the oxidation of  $\text{Li}_2\text{O}_2$  by  $\text{Br}_3^-$  in DMSO are reported in Figure 6.

In Figure 6a is evident the presence of the  $Br_3^-$  Raman signal before adding  $Li_2O_2$ . Its band shape is strongly different to that observed in ethers (see Figure 4a) and has the typical broad aspect of the  $Br_2$  signal (Figure S3), this is likely a consequence that the  $Br_3^-$  species exists mainly as a  $Br_2+Br^-$  complex. Always in Figure 6a can be appreciated as the consumption of  $Br_3^-$  was complete within few minutes from the starting of the reaction, indicating the very fast kinetics of the  $Li_2O_2$  oxidation by  $Br_3^-$  (or  $Br_2$ ) in DMSO. In Figure 6b are reported the DMA fluorescence spectra for the 1:1 reaction mixture with  $Br_3^-$  in DMSO before

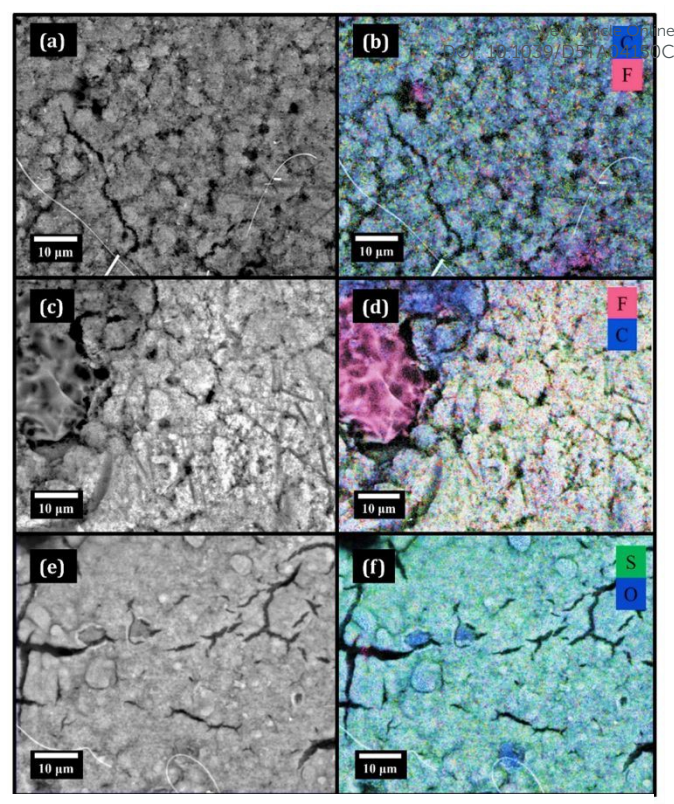


**Figure 7.** Scanning Electron Microscopy images (5.000x magnification, working distance of 8.44 mm, 15kV electron beam energy) of (a) GDL<sub>(DME)</sub>, (c) GDL<sub>(TEGDME)</sub>, (e) GDL<sub>(DMSO)</sub>. Corresponding EDX elemental mapping of (b) GDL<sub>(DME)</sub>, (d) GDL<sub>(TEGDME)</sub>, (f) GDL<sub>(DMSO)</sub>.

and after the addition of an excess of  $\text{Li}_2\text{O}_2$ , clearly indicating that the  $\text{Li}_2\text{O}_2$  oxidation is not accompanied by singlet oxygen evolution in this case. In fact, the fluorescence intensity of DMA is not affected by the occurrence of the reaction. This result is in perfect agreement with our previous considerations about the apparent need for a match between the Lewis character of the RM and the electrolyte solvent despite its polarity: DMSO is a strong Lewis acid characterized by a large acceptor number whereas  $\text{Br}_3^-$  is a weak Lewis base. Overall, LiBr redox mediation in DMSO, a high polarity solvent, seems to follow an alternative mechanism compared to low polarity ethers, that allows  $^1\text{O}_2$ -free  $\text{Li}_2\text{O}_2$  oxidation. In the case of DMSO, however, the performance outcome of LiBr as RM remains unsuccessful due to the solvent instability and to the formation during the charge not only of  $\text{Br}_3^-$ , but also of the more oxidizing  $\text{Br}_2$ .

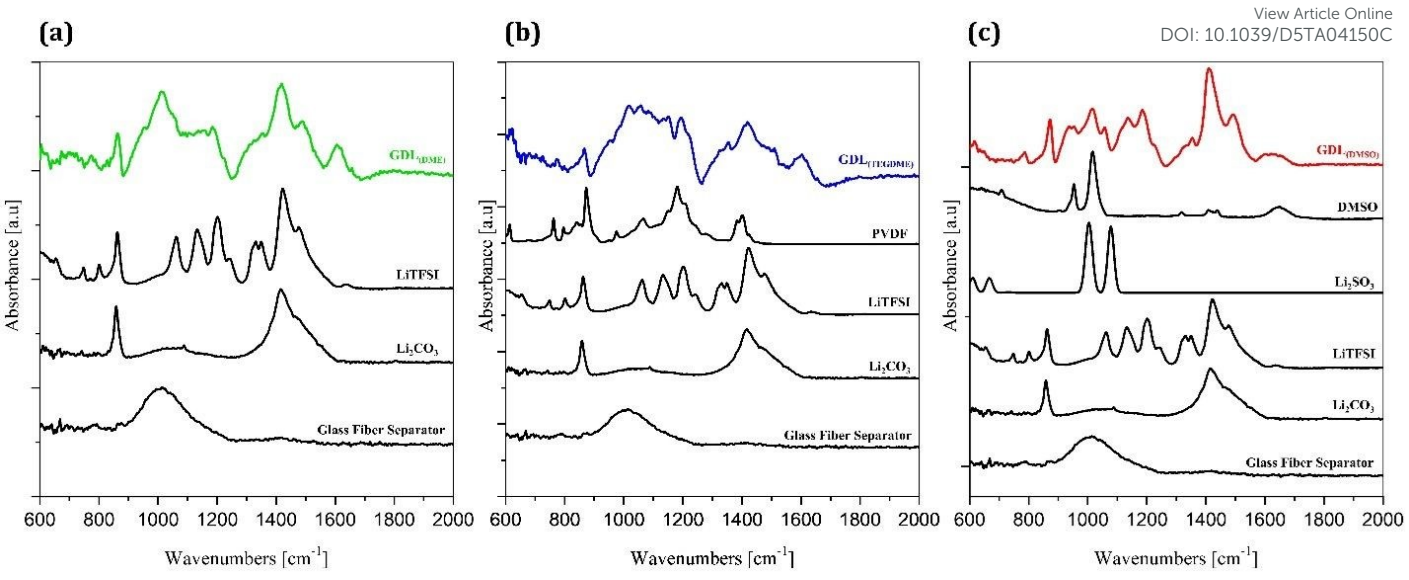
#### Post-mortem characterization of the positive electrodes.

Figure 7 reports the SEM images and corresponding EDX mapping of the Gas Diffusion Layers after their cycling in the DME, TEGDME and DMSO based electrolyte formulations, that will be referred to as  $GDL_{(DME)}$ ,  $GDL_{(TEGDME)}$  and  $GDL_{(DMSO)}$ , respectively.

In line with the electrochemical observations, GDL<sub>(DME)</sub> (Figure 7a and 7b) maintains a good morphology after cycling, similar to that of the pristine GDL (Figure S7), along with a clean surface free of significant deposits of degradation products. In fact, the EDX elemental mapping reported in Figure 7b and the

Open Access Article. Published on 21 October 2025. Downloaded on 10/27/2025 3:04:47 AM

Journal Name ARTICLE



**Figure 8.** ATR-FTIR spectra of (a) GDL<sub>(DME)</sub> and reference spectra of LiTFSI, Li<sub>2</sub>CO<sub>3</sub> and Whatman Glass Fiber separator. (b) GDL<sub>(TEGDME)</sub> and reference spectra of PVDF, LiTFSI, Li<sub>2</sub>CO<sub>3</sub> and Whatman Glass Fiber separator. (c) GDL<sub>(DMSO)</sub> and reference spectra of DMSO, Li<sub>2</sub>SO<sub>3</sub> (theoretical), LiTFSI, Li<sub>2</sub>CO<sub>3</sub> and Whatman Glass Fiber separator.

corresponding quantitative analysis (Table 1) indicate carbon as the main component, with small amounts of fluorine and sulfur that likely derive from the moderate degradation of the TFSI anion. GDL<sub>(DME)</sub> composition deviates less than the other postmortem samples respect to the composition of the pristine GDL (Table S2). The main difference lies in the oxygen content, increased after cycling, consistent with the formation of a natural Cathode-Electrolyte Interphase (CEI) formed from DME-derivates.

**Table 1.** EDX elemental quantitative analysis of Gas Diffusion Layers cycled with different electrolyte formulations.

	Atomic %						
Sample							
	С	0	S	F	Ni		
GDL <sub>(DME)</sub>	45.29	32.42	3.78	13.11	3.32		
GDL <sub>(TEGDME)</sub>	15.84	51.62	1.07	24.07	4.67		
GDL <sub>(DMSO)</sub>	24.72	53.19	13.10	6.48	1.64		

This picture is further supported by the ATR-FTIR spectrum of GDL<sub>(DME)</sub> (Figure 8a), where the main spectral features belong to TFSI<sup>-</sup> and Li<sub>2</sub>CO<sub>3</sub>, except for the band at  $\sim 1000~\text{cm}^{-1}$  ascribable to the -Si-O-Si- bonds of the glass fiber separator and to other minor components in the -C-O-C- region<sup>26</sup> belonging to ether-derived byproducts on the CEI.

In Figure 7c it is possible to observe that in the case of GDL<sub>(TEGDME)</sub>, after cycling, large portions of this cathode are constituted by amorphous and likely organic material, which appeared also to be very sensitive to the electron beam of the SEM microscope. From the EDX mapping (Figure 7d) and elemental quantification (Table 1) it was found that these regions are fluorine-rich, with no remarkable sulfur content. This hints that these byproducts are derived from the cathode polymeric binder, which is poly-vinylidenefluoride (PVDF). In

fact, the absence of significant amounts of S suggests that the degradation of LiTFSI, the only other source of fluorine apart from PVDF, is likely not involved at all in the formation of these deposits. The degradation of the polymeric binder leads to the loss of cathodic active material, i.e. carbon, in large parts of the cathode surface. The ATR-FTIR spectrum of GDL<sub>(TEGDME)</sub> is reported in Figure 8b and shows signals that match to those of PVDF and, to a minor extent, to LiTFSI. The small amounts of sulfur that are related to the LiTFSI-deriving byproducts appear located not in correspondence of the fluorine-rich deposits, but only on the remaining carbon surface (see Figure S8). Overall, from the characterization of the cycled cathode it is observed that the polymeric binder of the GDL is the cathode component that undergoes the majority of the undesired reactions occurring during the battery functioning.

The involvement of <sup>1</sup>O<sub>2</sub> in the degradation processes occurring on GLD(TEGDME) is likely, since carbon and PVDF are usually stable towards the other reactive species such as superoxide and peroxide, that are unavoidably formed during the battery operation in all the electrolyte formulations. This evidence is also in line with the recent findings of Zor et al. 26, that report no relevant <sup>1</sup>O<sub>2</sub>-related degradation of the electrolyte components from the characterization of the cycled cathode it is observed that the polymeric binder of the GDL is the cathode component that undergoes the majority of the undesired reactions occurring during the battery functioning. The involvement <sup>1</sup>O<sub>2</sub> in the degradation processes occurring on GDL(TEGDME) is likely, since carbon and PVDF are usually stable towards the other reactive species such as superoxide and peroxide, that are unavoidably formed during the battery operation in all the electrolyte formulations. This evidence is also in line with the recent findings of Zor et al.27, that report no relevant <sup>1</sup>O<sub>2</sub>-related degradation of the electrolyte components since neither TEGDME nor LiTFSI are affected by its presence.

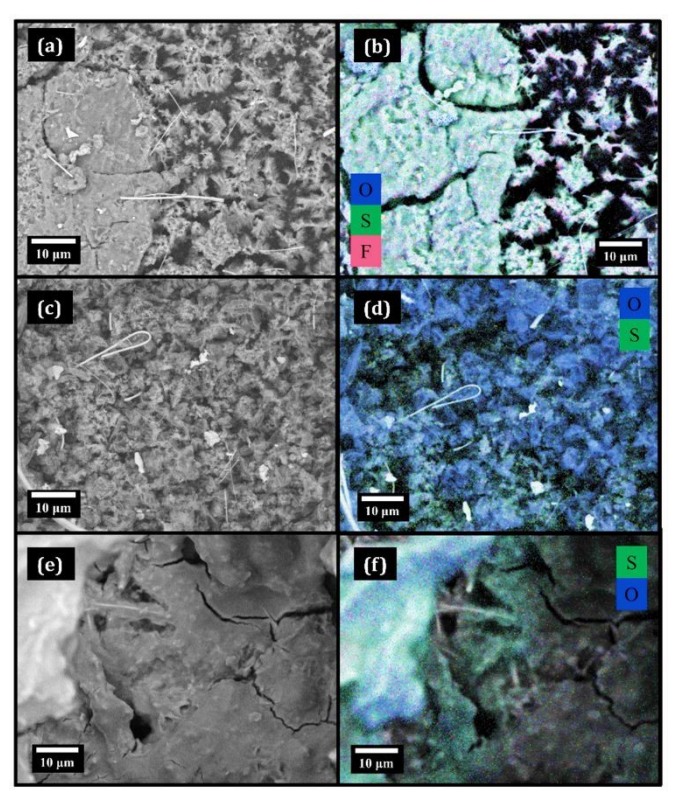


**Figure 9.** Scanning Electron Microscopy images (5.000x magnification, working distance of 8.44 mm, 15kV electron beam energy) of (a) Li<sub>(DME)</sub>, (c) Li<sub>(TEGDME)</sub>, (e) Li<sub>(DMSO)</sub>. Corresponding EDX elemental mapping of (b) Li<sub>(DME)</sub>, (d) Li<sub>(TEGDME)</sub>, (f) Li<sub>(DMSO)</sub>.

This implies that in case of  $^1\text{O}_2$  evolution the other cell components, including the electrode binder, would be preferentially attacked.

The SEM images and EDX elemental maps of  $\mathsf{GDL}_{(\mathsf{DMSO})}$  are reported in Figure 7e and 7f and confirm the accumulation of byproducts during the battery operation. The surface of the GDL is covered by a thick film-like layer mainly formed by the degradation of DMSO and secondarily TFSI-, according to the relative quantities of S and F detected by EDX elemental quantification (Table 1). The Cathode-Electrolyte Interphase is composed of uniformly-distributed sulfur and localized oxygenrich regions (Figure 7f). In the ATR-FTIR spectrum of GDL(DMSO) (Figure 8c) the diagnostic signal of S=O stretching at 1044 cm<sup>-1</sup> <sup>28</sup> is intense, indicating the presence of other DMSO-related byproducts. Among them, Li<sub>2</sub>SO<sub>3</sub> is likely to be present since there are compatible peaks between 900 and 1100 cm<sup>-1</sup> in the sample spectrum. The presence of dimethyl sulfide and methanesulfonic acid, the main byproducts expected by the Br<sub>2</sub> induced decomposition of DMSO<sup>25</sup>, is also compatible with the GDL(DMSO) spectrum as highlighted in Figure S9.

#### Post-mortem characterization of the negative electrodes.

Figure 9 shows the morphology and elemental mapping by SEM/EDX of Li metal anodes after cycling in the different electrolytes, hereafter referred to as  $Li_{(DME)}$ ,  $Li_{(TEGDME)}$  and  $Li_{(DMSO)}$ .

In Figure 9a, the SEM image of Li<sub>(DME)</sub> clearly shows the anode deterioration with the presence of Cendrities structures, indicating a less than optimal anode functioning in the DME-based electrolyte. In analogy with other Li metal battery systems, in Li-O<sub>2</sub> cells dendrites lead to Li detachment and loss of electrical contact that compromise the cell functioning, constituting at the same time a severe safety hazard due to the possibility of short circuits<sup>29</sup>. The corresponding EDX elemental mapping in Figure 9b indicates oxygen-rich regions, hinting that the degradation of the ether solvent occurred. The significant amounts of S and F on the Li surface (see Table 2) indicate also the presence of TFSI- fragments in the Solid Electrolyte Interphase (SEI).

The morphology of Li(TEGDME) in Figure 9c appears different, showing predominantly mossy lithium. Thus, also in this case the uniformity of the Li morphology is compromised after the battery cycling, but the composition of the SEI layer is remarkably better in respect to the Li(DME) case. In fact, both the elemental mapping (Figure 9d) and the quantitative analysis (Table 2) show oxygen as the major component. Usually, the presence of oxygen matches that of lithium, an element that cannot be detected by EDX spectroscopy. Thus, a rich and relatively uniform mapping of oxygen on the Li metal anode suggests the presence of a very thin SEI layer originated from byproducts formed by the reactions of Li with the electrolyte. Few amounts of S and F on the Li surface indicate mild TFSIdegradation that always occurs during the formation of the natural SEI layer on Li anodes. The improved stability of the TEGDME-based electrolyte towards Li metal respect to the DME case is explained by the TEGDME tendency to complex Li<sup>+</sup> within the LiTFSI ionic couple thanks to its longer chain<sup>30</sup>. This intermolecular interaction has been already demonstrated to play a key role in protecting the ether from oxidation<sup>31</sup>, i.e. the hydrogen abstraction from methylene groups by nucleophilic agents<sup>32</sup>.

The Li<sub>(DMSO)</sub> anode (Figure 9e) shows some separator fibers that are incorporated in a thick film, mainly composed by S and O (Figure 9f). Significant quantities of carbon are also present in the electrode surface (Table 2), supporting the occurrence of severe degradation of electrolyte components. As in the case of GDL<sub>(DMSO)</sub>, the relative amount of S is higher than that of F, indicating that sulfur-containing byproducts derive mostly from DMSO. The Li metal anode appears consumed in the parasitic processes and covered with an insulating film that affects the reversibility of the plating/stripping processes.

**Table 2.** EDX elemental quantitative analysis of lithium metal anodes cycled with different electrolyte formulations.

Sample	Atomic %						
	С	0	S	F	Ni		
Li <sub>(DME)</sub>	36.09	16.58	10.67	32.10	3.49		
Li <sub>(TEGDME)</sub>	12.75	76.36	2.79	6.94			
Li <sub>(DMSO)</sub>	46.17	20.20	17.75	11.70	3.67		

#### Conclusion

This article is licensed under a Creative Commons Attribution-NonCommercial 3.0 Unported Licence

Article. Published on 21 October 2025. Downloaded on 10/27/2025 3:04:47 AM

Journal Name ARTICLE

Employing LiBr as redox mediator in Li- $O_2$  batteries leads to radically different outcomes varying the solvent media. The optimal reversibility of cathodic reactions, i.e. ORR and OER, is obtained in DME, while critical issues rise in both the other solvents, i.e. TEGDME and DMSO. The cathode functioning in TEGDME is affected by  $^1O_2$ -induced parasitic processes. Conversely, in DMSO LiBr redox mediation appears to follow a different mechanism allowing  $^1O_2$ -free OER but, at the same time, enabling DMSO decomposition induced by Br<sub>2</sub>. The Li metal anode functioning is not directly correlated to the cathode operation, since the worst Li morphology was found in the DME case. This implies that Li metal protection must be addressed independently.

In summary our study underscores the critical role of solvent effects on the intricate interplay between the redox mediator, lithium superoxide (LiO<sub>2</sub>), and the TFSI<sup>-</sup> anion in dictating singlet oxygen (1O<sub>2</sub>) release pathways in Li-O<sub>2</sub> batteries. It is well known that the choice of solvent significantly influences the solvation of these species, affecting the redox potentials, ion pairing, and overall electrochemical stability of the electrolyte. Specifically, the degree of Lewis acidity and basicity of the solvent, coupled with its dielectric constant, dictates the extent to which LiO<sub>2</sub> and TFSI<sup>-</sup> are solvated, subsequently influencing the reaction kinetics and the propensity for <sup>1</sup>O<sub>2</sub> generation. A mismatch in the Lewis characteristics of the solvent and redox mediator can promote parasitic reactions and the formation of <sup>1</sup>O<sub>2</sub>, ultimately contributing to cell degradation. Understanding and tailoring the solvation environment is therefore crucial for suppressing <sup>1</sup>O₂ formation and optimizing the performance and lifespan of Li-O<sub>2</sub> batteries. Therefore, the most promising approach for a reversible operation of an aprotic Li-O<sub>2</sub> battery is the employment of RM with Lewis basicity contrasting the corresponding Lewis acidity of the electrolyte solvent, in parallel with a tailored Li metal protection strategy the limits the parasitic chemistries originating at the negative side.

#### **Author contributions**

All authors contributed equally t this work

#### **Conflicts of interest**

"There are no conflicts to declare".

#### Data availability

Data for this article, including raw spectral data, electrochemical data, microscopy images, are available at SAPIENZA Open DATA, at <a href="https://doi.org/10.13133/UNIROMA1/TAIQ8Y">https://doi.org/10.13133/UNIROMA1/TAIQ8Y</a>.

### Acknowledgements

This research work has been supported by the University of Rome La Sapienza through the grants RM12117A7572D7AD, RM12218166CCF3CC and by the "Progetto Orangees -

ORgANics for Green Electrochemical Energy Storage ATTIC CODICE CSEAA\_00010" funded by the Italian Government Through the MITE (Ministero della Transizione Ecologica) call 2022 "Bandi di gara di tipo A". EB and AP also acknowledge the financial support of "La Sapienza" with grants n. RM1221814C52ED98, AR1231888A2B7002, AR1221816B8CBDBA and the support from CINECA with grant IsB30\_PFEX.

#### References

- **1.** Kwak, W.-J., Rosy, Sharon, D., Xia, C., Kim, H., Johnson, L.R., Bruce, P.G., Nazar, L.F., Sun, Y.-K., Frimer, A.A., Noked, M., Freunberger, S.A., Aurbach, D., Lithium-Oxygen Batteries and Related Systems: Potential, Status, and Future, **2020**, *ACS Appl. Mater. Interfaces*, 120, 14, 6626-6683, DOI: 10.1021/acs.chemrev.9b0060.
- **2.** Zakharchenko, T. K., Sergeev, A.V., Bashkirov, A.D., Neklyudova, P., Cervellino, A., Itkis, D.M., Yashina, L.V., Homogeneous nucleation of Li<sub>2</sub>O<sub>2</sub> under Li-O<sub>2</sub> battery discharge, **2020**, *Nanoscale*, 12, 4591–4601, DOI: 10.1039/C9NR08493B.
- **3.** Varzi, A., Thanner, K., Scipioni, R., Di Lecce, D., Hassoun, J., Dorfler, S., Altheus, H., Kaskel, S., Prehal, C., Freunberger, S.A., Current status and future perspectives of lithium metal batteries, **2020**, *J. Power Sources*, 480, 228803, DOI: 10.1016/j.jpowsour.2020.228803.
- **4.** Pierini, A., Brutti, S., Bodo, E., Reactive pathways toward parasitic release of singlet oxygen in metal-air batteries, **2021**, *npj Comput. Mater.*, **71**, **7**, **1-8**, DOI: 10.1038/s41524-021-00597-3.
- **5.** Jiang, Z., Huang, Y., Zhu, Z., Li, F., Quenching singlet oxygen via intersystem crossing for a stable Li-O<sub>2</sub> battery, **2022**, *Proc. Natl. Acad. Sci. U.S.A.*, 119 (34), e2202835119, DOI: 10.1073/pnas.2202835119.
- **6.** Jiang, Z., Wen, B., Huang, Y., Wang, Y., Fang, H., Li, F., Heavy Atom-Induced Spin-Orbit Coupling to Quench Singlet Oxygen in a Li-O<sub>2</sub> Battery, **2025**, *J. Am. Chem. Soc.*, 147, 13, 10992-10998.
- **7.** Chen, Y., Freunberger, S. A., Peng, Z., Fontaine, O., Bruce, P. G., Charging a Li-O₂ battery using a redox mediator, **2013**, *Nat. Chem.* 5, 489–494, DOI: 10.1038/nchem.1646.
- **8.** Gao, X., Chen, Y., Johnson, L. R., Jovanov, Z. P., Bruce, P. G., A rechargeable lithium—oxygen battery with dual mediators stabilizing the carbon cathode, **2017**, *Nat. Energy*, 2, 17118, DOI: 10.1038/nenergy.2017.118.
- **9.** Zhang, C., Dandu, N., Rastegar, S., Misal, S.N., Hemmat, Z., Ngo, A.T., Curtiss, L.A., Salehi-Khojin, A., A Comparative Study of Redox Mediators for Improved Performance of Li-Oxygen Batteries, **2020**, *Adv. Energy Mater.* 10, 2000201, DOI: 10.1002/aenm.202000201.
- **10.** Leverick, G., Feng, S., Acosta, P., Acquaviva, S., Bardé, F., Cotte, S., Shao-Horn, Y., Tunable Redox Mediators for Li– $O_2$  Batteries Based on Interhalide Complexes, **2022**, *ACS Appl. Mater. Interfaces*, 14, 6689-6701, DOI: 10.1021/acsami.1c21905.
- **11.** Nakanishi, A., Thomas, M.L., Kwon, H.-M., Kobayashi, Y., Tatara, R., Ueno, K., Dokko, K., Watanabe, M., Electrolyte

Shemistry A Accepted

**ARTICLE Journal Name** 

Composition in Li/O<sub>2</sub> Batteries with LiI Redox Mediators: Solvation Effects on Redox Potentials and Implications for Redox Shuttling, 2018, J. Phys. Chem. C, 122, 1522-1534, DOI: 10.1021/acs.jpcc.7b11859.

- 12. Leverick, G., Tułodziecki, M., Tatara, R., Bardé, F., Shao-Horn, Y., Solvent-Dependent Oxidizing Power of Lil Redox Couples for Li-O<sub>2</sub> Batteries, 2019, Joule, 3, 1106-1126, DOI: 10.1016/j.joule.2018.12.014.
- 13. Wang, A., Wu, X., Zou, Z., Qiao, Y., Wang, D., Xing, L., Chen, Y., Lin, Y., Avdeev, M., Shi, S., The Origin of Solvent Deprotonation in Lil-added Aprotic Electrolytes for Li-O<sub>2</sub> Batteries, 2023, Angew. Chemie - Int. Ed., 62(14), DOI: 10.1002/anie.202217354.
- 14. Kwak, W.-J., Hirshberg, D., Sharon, D., Afri, M., Frimer, A.A., Jung, H.-G., Aurbach, D., Sun, Y.-K., Li-O₂ cells with LiBr as an electrolyte and a redox mediator, 2016, Energy Environ. Sci., 9, 2334-2345, DOI:10.1039/C6EE00700G.
- 15. Pierini, A., Petrongari, A., Piacentini, V., Brutti, S., Bodo, E., A Computational Study on Halogen/Halide Redox Mediators and Their Role in <sup>1</sup>O<sub>2</sub> Release in Aprotic Li-O<sub>2</sub> Batteries, **2023**, *J.* Phys. Chem. Α, 127, 44, 9229-9235, DOI:10.1021/acs.jpca.3C05246.
- 16. Petrongari, A., Pierini, A., Piacentini, V., Fattibene, P., De Angelis, C., Bodo, E., Brutti, S., Insights into the Lil Redox Mediation in Aprotic Li-O<sub>2</sub> Batteries: Solvation Effects and Singlet Oxygen Evolution, 2023, ACS Appl. Mater. Interfaces, 15, 51, 59348-59357, DOI: 10.1021/acsami.3c12330.
- 17. Riadigos, C. F., Iglesias, R., Rivas, M. A., Iglesias, T. P., Permittivity and density of the systems (monoglyme, diglyme, triglyme, or tetraglyme + n-heptane) at several temperatures, Chem. 2011, J. Thermodyn. 275-283, DOI:10.1016/j.jct.2010.09.008.
- 18. Ponrouch, A., Marchante, E., Courty, M., Tarascon, J. M., Palacín, M. R., In search of an optimized electrolyte for Na-ion batteries, 2012, Energy Environ. Sci., 5, 8572-8583, DOI: 10.1039/C2EE22258B.
- 19. Jezuita, A., Wieczorkiewicz, P. A., Szatylowicz, H., Krygowski, T. M., Solvent effect on the stability and reverse substituent effect in nitropurine tautomers, 2021, Symmetry, 13, 1223, DOI: 10.3390/sym13071223.
- 20. Chai, J.-D., Head-Gordon, M., Long-range corrected hybrid density functionals with damped atom-atom dispersion corrections, 2008, Phys. Chem. Chem. Phys. 10, 6615-6620, DOI: 10.1039/B810189B.
- 21. Neese, F., Software update: The ORCA program system— Version 5.0, 2022, WIREs Comput. Mol. Sci., 12, e1606, DOI: 10.1002/wcms.1606.
- 22. Ahmadiparidari, A., Fuladi, S., Majidi, L., Plunkett, S., Sarnello, E., Gholivand, H., Hemmat, Z., Rastegar, S., Misal, S.N., Jimenez, N., Redfern, P.C., Wen, J., Li, T., Ngo, A.T., Khalili-Araghi, F., Curtiss, L.A., Salehi-Khojin, A., Enhancing the performance of lithium oxygen batteries through combining redox mediating salts with a lithium protecting salt, 2021, J. Power Sources, 491, DOI: 10.1016/j.jpowsour.2021.229506.
- 23. Lin, M., Archirel, P., Thi Van-Oanh, N., Muroya, Y., Fu, H., Yan, Y., Nagaishi, R., Kumagai, Y., Katsumura, Y., Mostafavi, M., Temperature dependent absorption spectra of Br<sup>-</sup>, Br<sub>2</sub><sup>•</sup>, and Br<sub>3</sub><sup>-</sup>

- in aqueous solutions, 2011, J. Phys. Chem. A 115, 4241 4247 DOI: 10.1021/jp1123103.
- 24. Kwak, W.-J., Kim, H., Jung, H.-G., Aurbach, D., Sun, Y.-K. Review—A Comparative Evaluation of Redox Mediators for Li-O2 Batteries: A Critical Review, 2018, J. Electrochem. Soc., 165, A2274-A2293, DOI: 10.1149/2.0901810jes.
- 25. Aida, T., Akasaka, T., Furukawa, N., Oae, S. Catalytic Reduction of Sulfoxide by Bromine-Hydrogen Bromide System, 1976, Bull. Chem. Soc. Jpn., 49, 1117-1121, DOI: 10.1246/bcsj.49.1117.
- 26. Papke, B. L., Ratner, M. A., Shriver, D. F., Vibrational spectroscopy and structure of polymer electrolytes, poly(ethylene oxide) complexes of alkali metal salts, 1981, J. Phys. Chem. Solids, 42, 493-500, DOI: 10.1016/0022-3697(81)90030-5.
- 27. Zor, C., Jones, K.D., Rees, G. J., Yang, S., Pateman, A., Gao, X., Johnson, L. R., Bruce, P. G., Singlet oxygen is not the main source of electrolyte degradation in lithium-oxygen batteries, Energy Environ. 7355-7361, 2024. Sci., 17, 10.1039/D4EE02176B.
- 28. Ravi, J., Hills, A., Cerasoli, E., Rakowska, P. D., Ryadnov, M. G., FTIR markers of methionine oxidation for early detection of oxidized protein therapeutics, 2011, Eur. Biophys. J., 40, 339-345, DOI: 10.1007/s00249-010-0656-1.
- 29. Hong, Y.-S., Zhao, C.-Z., Xiao, Y., Xu, R., Xu, J.-J., Huang, J.-Q., Zhang, Q., Yu, X., Li, H., Safe Lithium-Metal Anodes for Li-O<sub>2</sub> Batteries: From Fundamental Chemistry to Advanced Characterization and Effective Protection, 2019, Batter. Supercaps, 2, 638-658, DOI: 10.1002/batt.201900031.
- 30. Adams, B. D., Black, R., Williams, Z., Fernandes, R., Cuisinier, M., Jaemstorp Berg, E., Novak, P., Murphy, G. K., Nazar, L. F., Towards a Stable Organic Electrolyte for the Lithium Oxygen Battery, 2015, Adv. Energy Mater., 5, 1400867, DOI: 10.1002/aenm.201400867.
- 31. Tsuzuki, S., Shinoda, W., Seki, S., Umebayashi, Y., Yoshida, K., Dokko, K., Watanabe, M., Intermolecular Interactions in Li+glyme and Li+-glyme-TFSA- Complexes: Relationship with Physicochemical Properties of [Li(glyme)][TFSA] Ionic Liquids, 2013, ChemPhysChem, 14, 1993-2001, 10.1002/cphc.201200843.
- 32. Carboni, M., Marrani, A. G., Spezia, R., Brutti, S., 1,2-Dimethoxyethane Degradation Thermodynamics in Li-O2 Redox Environments, 2016, Chem. - A Eur. J., 22, 17188-17203, DOI:10.1002/chem.201602375.

# **DATA AVAILABILITY**

View Article Online DOI: 10.1039/D5TA04150C

Data for this article, including raw spectral data, electrochemical data, microscopy images, are available at SAPIENZA Open DATA, at <a href="https://doi.org/10.13133/UNIROMA1/TAIQ8Y">https://doi.org/10.13133/UNIROMA1/TAIQ8Y</a>